ELSEVIER

Journal of Marine Systems 29 (2001) 277–292

JOURNAL OF MARINE SYSTEMS

www.elsevier.nl/locate/jmarsys

Surface distribution of chlorophyll, particles and gelbstoff in the Atlantic jet of the Alborán Sea: from submesoscale to subinertial scales of variability

J. Ruiz [a,*], F. Echevarría [a], J. Font [b], S. Ruiz [b], E. García [b], J.M. Blanco [c], F. Jiménez-Gómez [c], L. Prieto [a], A. González-Alaminos [a], C.M. García [a], P. Cipollini [d], H. Snaith [d], A. Bartual [a], A. Reul [c], V. Rodríguez [c]

[a] *Área de Ecología, Departamento de Biologia y Ecologia, Facultad de Ciencias del Mar, Universidad de Cádiz, Apartado, num. 40, 11510-Puerto Real, Cádiz, Spain*

[b] *Institut de Cienciés del Mar, Passeig Joan de Borbo s / n, 08039 Barcelona, Spain*

[c] *Departamento de Ecología, Facultad de Ciencias, Universidad de Málaga, 29071 Málaga, Spain*

[d] *Southampton Oceanography Centre SO14 3ZH, UK*

Received 1 August 1999; accepted 12 September 2000

Abstract

The surface distribution of light attenuation due to particles (c) as well as chlorophyll-*a* and gelbstoff fluorescence (F_{ch} and F_{cd}, respectively) were recorded during an OMEGA (EU funded, MAST III project) cruise in the northwestern Alborán Sea through a high spatial (zonally separated by 10 km and virtually meridionally continuous) and temporal (about 3 days between each of the three repeated surveys made in the zone) resolution sampling design. The distributions obtained for these variables were tightly linked to the physical forcing at the different scales that the sampling design was able to resolve. Low values dominate the quasi permanent anticyclonic gyre occupying the western Alborán Sea, whereas the frontal zone directly affected by the entrance of the Atlantic jet depicts much higher records for c, F_{ch} and F_{cd}.

High geostrophic Froude numbers in the jet, and the subsequent increase in turbulence diffusion of nutrients towards the surface, cannot alone justify this spatial distribution. Instead, high phytoplankton concentration at the jet could also result from the entrainment and advection of water from the upwelling zone at the Spanish coast. However, T–S characteristics suggest that this is neither the most important process for the biological enrichment of the jet, so that other mechanisms such as vertical ageostrophic velocities at the edge of the gyre must also be considered. Due to the time needed for phytoplankton growth, the intense horizontal velocities associated to the jet can decouple the sectors where deep nutrient-rich waters reach the surface from sectors where high values of the recorded variables are observed. The decoupling hinders a differentiation of this fertilization mechanism from other possible alternatives as mixing at the sills in the Strait of Gibraltar.

In the third survey, the spatial structure of surface warm waters in the gyre and cold waters in the front became less apparent. ADCP data show a southward migration of the jet in a fluctuation probably related to transient states in the Atlantic jet and western Alborán gyre system. The qualitative response of c, F_{ch} and F_{cd} to these scales of variability was

* Corresponding author. Tel.: +34-56-470-836; fax: +34-956-016-019.
E-mail address: Javier.Ruiz@uca.es (J. Ruiz).

PII: S0924-7963(01)00020-3

very similar and close to the changes observed in temperature. However, the values of F_{cd} varied in a much narrower range than c or F_{ch} (a factor of 2 and 10, respectively), which indicates a distinct control for the abundance of Gelbstoff. This control dumps the range of variability in the western Alborán and its origin is discussed in the context of photobleaching or bacterial degradation of these substances.

Keywords: Alborán Sea; Mesoscale; Submesoscale; Physical forcing of biology; Continuous recording; Surface biological signals

1. Introduction

The western Alborán sea is a highly dynamic area due to the kinetic energy associated to the incoming jet of Atlantic waters. This flow generates a quasi permanent anticyclonic gyre adjacent to the Gibraltar Strait and a less permanent gyre at the eastern part of the basin (Lanoix, 1974; Arnone et al., 1990; La Violette, 1984; Vazquez-Cuervo et al., 1996). The high velocity (in the range of 1 m/s) characteristic of the jet and the small Rossby radius of deformation of the zone (20 km; Tintoré et al., 1991) make this

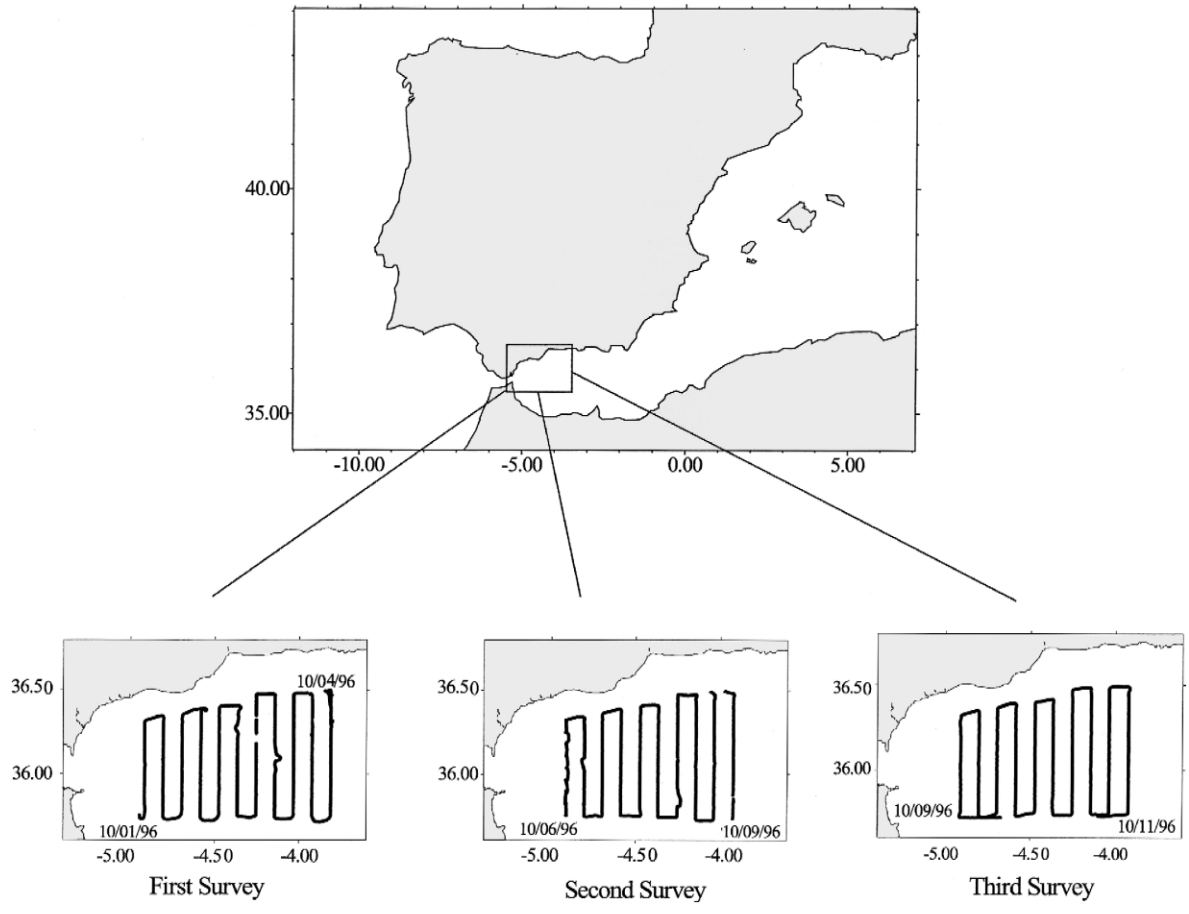

Fig. 1. Track followed by the vessel during the three surveys. The start and end time for each survey are also shown.

area also subjected to very intense mesoscale (Tintoré et al., 1991; Viúdez et al., 1996) and submesoscale (La Violette, 1984) variability. This dynamic character is translated to a pelagic community that shows sharp gradients and rapid changes in the concentration as well as in the composition and size structure of phytoplankton populations (Rubín et al., 1992; Prieto et al., 1999; Rodríguez et al., 1998; Prieto et al., in press). The variability is so intense that the different spatial and temporal scales at which the coupling between physical forcing and pelagic response takes place can barely be resolved through a standard station-by-station biochemical sampling program. This is positively the case for mesoscale processes, which under this sampling design, appear as atypical stations whose results are difficult to interpret in the context of more permanent features present in the zone (Prieto et al., 1999; Vargas Yáñez et al., 1999). To resolve these sources of variability, it is desirable to have an effort for increasing the spatial and temporal resolution as well as the synopticity of the data. The results presented in this paper undertake this objective when recording the distribution of biological and chemical variables in the northwestern Alborán Sea.

They include the surface distribution for estimators of particles, chlorophyll and chromophore-containing dissolved organic matter concentration. The

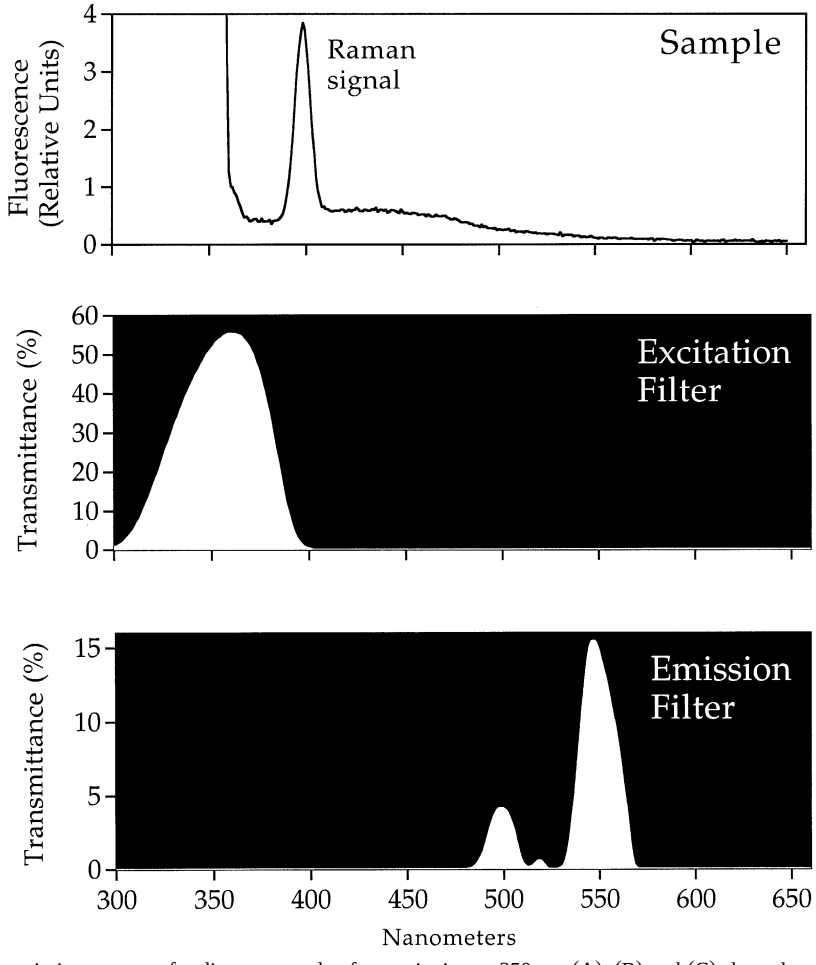

Fig. 2. Example of the emission spectra of a discrete sample after excitation at 350 nm (A). (B) and (C) show the transmittance spectra of excitation and emission filters respectively installed in the Turner fluorometer for F_{cd} measurement.

high spatial (zonally separated by 10 km and meridionally continuous) and temporal (about 3 days) resolution of the results makes them an interesting example of pelagos dynamics in highly dynamic areas and a singular analysis of the zone. They have allowed to show the tight control that physical forcing has on the pelagos that occupies the Alborán Sea directly affected by the entrance of the Atlantic jet. A control manifested at the different scales that the sampling design was capable of resolving, from submesoscale features to more scarce subinertial events related to transient states in the Atlantic jet and western Alborán gyre system.

2. Material and methods

Data were obtained in October 1996, during the cruise OMEGA on board the oceanographic vessel Hespérides. An area of about 100×80 km^2 covering the north section of the anticyclonic Alborán Sea gyre was surveyed three times with a time lag between two consecutive surveys of about 4 (first and second) or 2 (second and third) days. The location of the area and the track followed by the vessel in each survey is presented in Fig. 1. The three surveys were made in the west to east direction (after each survey the vessel returned to the initial point) in a downstream flow sampling strategy. Consequently, a relaxation of the recorded (with respect to the real) spatial gradients associated to non-stationary eastward propagating structures of size larger than the jet width can be expected. For small structures within the jet, we must take into account their high eastward propagation (in the order of 1 m/s), the fact that for most of the time the vessel followed a meridional course, and the distance (about 12 km) between transects. With these elements, our sampling strategy only allows to rely in meridional gradients for the surface distribution of biological signals within the jet, since their recording along a transect is almost synchronous. This is not the case for zonal gradients within the jet. Due to the course followed by the vessel, the same distance between two points where a biological signal is recorded implies a longer time span if these points belong (as necessary to construct zonal gradients) to different transects. For non-stationary biological structures that are very rapidly displaced within the jet, this means the possibility of a distortion in the recorded zonal structures.

The pumping system of the Hespérides was connected to a SeaBird thermosalinograph and a Turner® fluorometer for the determination of chlorophyll fluorescence. In addition, a Wet Labs C Star® transmissometer with a 25-cm path length and a light of 660 nm was also installed for the recording of light beam attenuation due to particle scattering. Discrete samples for the determination of chlorophyll and particle volume concentration were also obtained while the vessel was underway (Fig. 1). Chlorophyll was measured by the fluorometric method of Yentsch and Menzel (1963) and particle concentration was determined with a Coulter Counter Multisizer II®

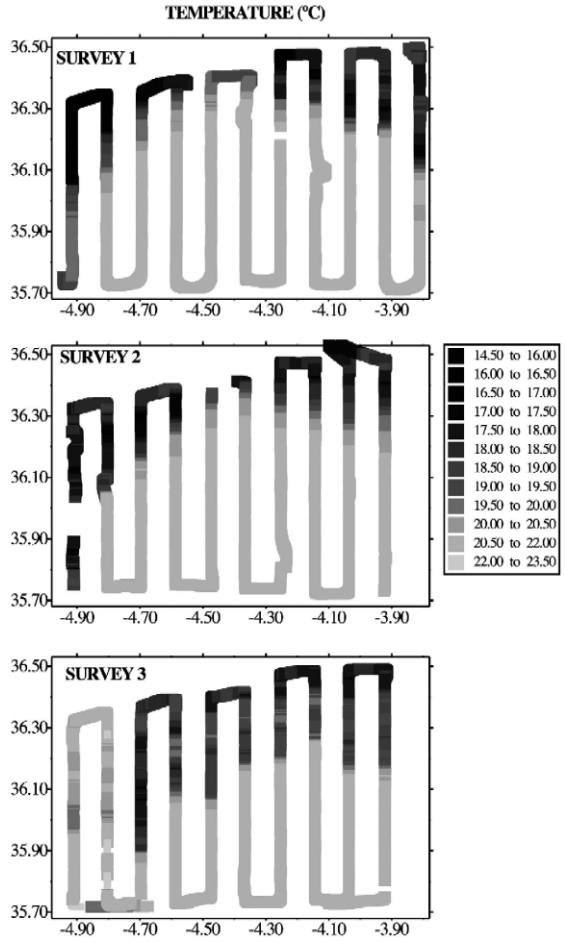

Fig. 3. Surface distribution of temperature (°C) in the three surveys.

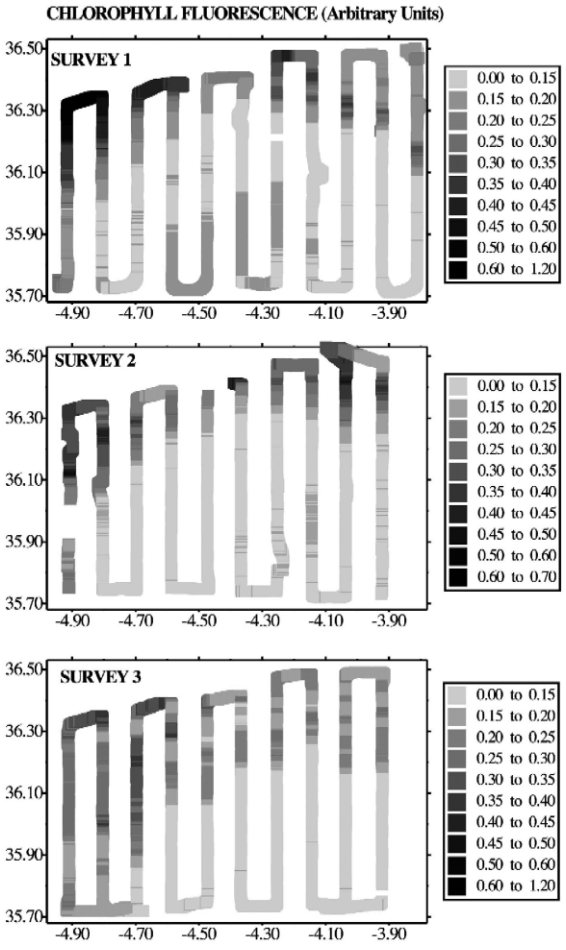

Fig. 4. Surface distribution of F_{ch} (arbitrary units) in the three surveys.

provided with a 140-μm tube. This concentration is expressed in milligrams per liter of particles within the size range from 3 to 40 μm of equivalent spherical diameter. Size spectra of plankton were also obtained for some of these discrete samples following the methods described by Rodríguez and Li (1994).

Another Turner fluorometer was also installed but with a lamp, excitation and emission filters adequate for chromophore-containing dissolved organic matter (CDOM) fluorescence recording. When excited under ultraviolet, the CDOM emits light in a broad band of wavelengths within the visible range. The emission spectra also contains an important Raman signal in wavelengths close to that of excitation (Kirk, 1994) that could mask the CDOM signal. The excitation and emission filters (numbers 10–069 and 10–056 of Turner catalog, respectively) as well as the lamp (10–047) installed in the fluorometer form a combination that allows excitation in the ultraviolet while recording emission in a waveband not very heavily affected neither by the Raman signal nor by chlorophyll fluorescence. The transmitance spectra of both filters is shown in Fig. 2. This figure also shows an example of the emission spectra of a discrete sample as recorded by a spectrofluorometer after excitation at 350 nm, within the transparent range of the Turner excitation monochromator. Milli-

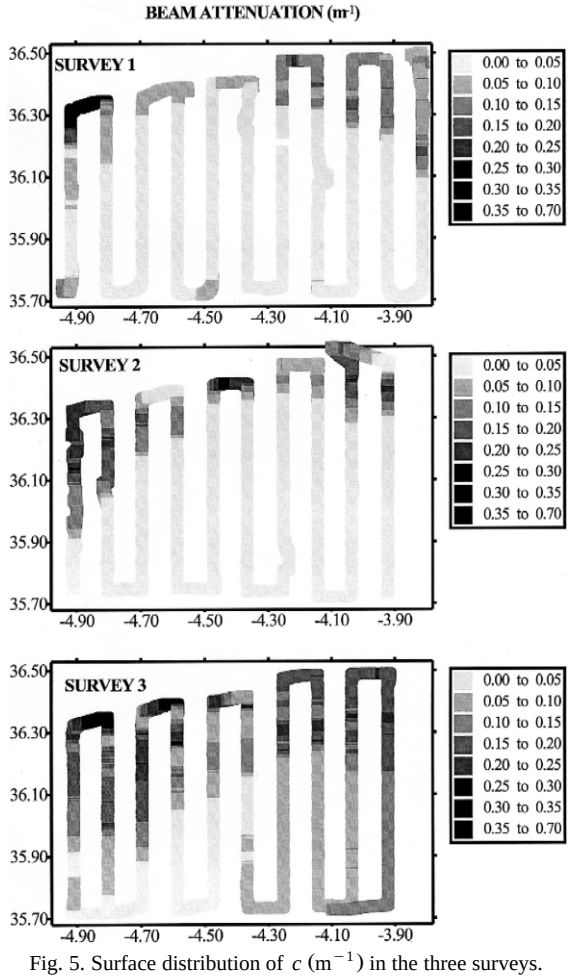

Fig. 5. Surface distribution of c (m^{-1}) in the three surveys.

Q water was used as blank and a solution of quinine sulfate in H_2SO_4 as a fluorescence standard to report data as fluorescence standard units (Hoge et al., 1993; Vodacek et al., 1997). The association of this fluorescence signal and absorbance of CDOM was determined for several discrete samples. These were filtrated by Millipore APFF and the absorption spectra were obtained with a Beckman® spectrophotometer provided with a 10-cm quartz cell.

The output voltage from both fluorometers (chlorophyll and CDOM fluorescence) and from transmissometer was digitized through an analog-to-digital converter with a very high sampling rate. An average of 1000 registers from this digitizer, recorded in a period of about 1 s, was taken every half minute and averaged prior to storing the data in a file. Very stable and reliable signals were recorded with this method during the cruise. These data were then merged with temperature from the vessel thermosalinograph. Noisy conductivity records prevented the further use of salinity from this equipment. Punctual salinity records from a towed Seasoar as well as surface ADCP velocity data are also presented when necessary to discuss the surface distribution of biological signals in the area.

3. Results

The presence of the anticyclonic gyre and a front of cold waters in the zone is clearly traced by the sea surface temperature distribution during the first and second surveys whereas this feature is not so sharp in the third survey (Fig. 3). Temporal changes in the spatial distribution of variables among the different surveys evidence the highly dynamic character of the zone. The change is especially apparent between the second and third survey, with a laxer frontal structure in the last case. The distribution of other variables like chlorophyll fluorescence (F_{ch}) and beam attenuation coefficient (c) is similar to that of temperature. In both cases, the higher values are found in the north and west where temperature is lower, and a more vague structure is observed in the third survey (Figs. 4 and 5). In the first survey, there is also a coincidence of very low temperatures in the northwestern part of the area with very high values of c and F_{ch}. This zone is usually occupied by cold surface waters, a feature that results from the formation of a cyclonic gyre north to the front (Vazquez-Cuervo et al., 1996) and is inforced when sustained westerly winds blow at the zone (Minas et al., 1987). This situation occurred during the days previous to the first survey (Fig. 6) and, as revealed by the AVHRR thermal image (Plate 1A), very cold waters occupied the surface of the northwestern Alborán Sea during that period.

There is scatter in the plot of c and F_{ch} versus particles and chlorophyll concentration respectively (Fig. 7) and, therefore, c and F_{ch} cannot be considered as perfectly accurate estimators. Thus, changes in c and F_{ch} are not only due to changes in the concentration of the variables they assess, but also a result of differences in the optical characteristics of

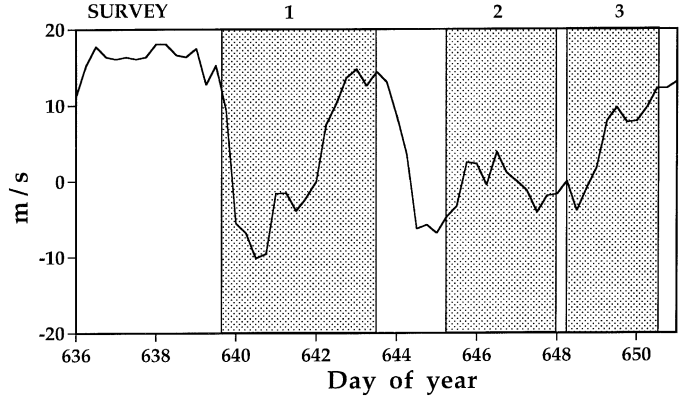

Fig. 6. Zonal component of wind in Tarifa. Positive values of wind are westerlies.

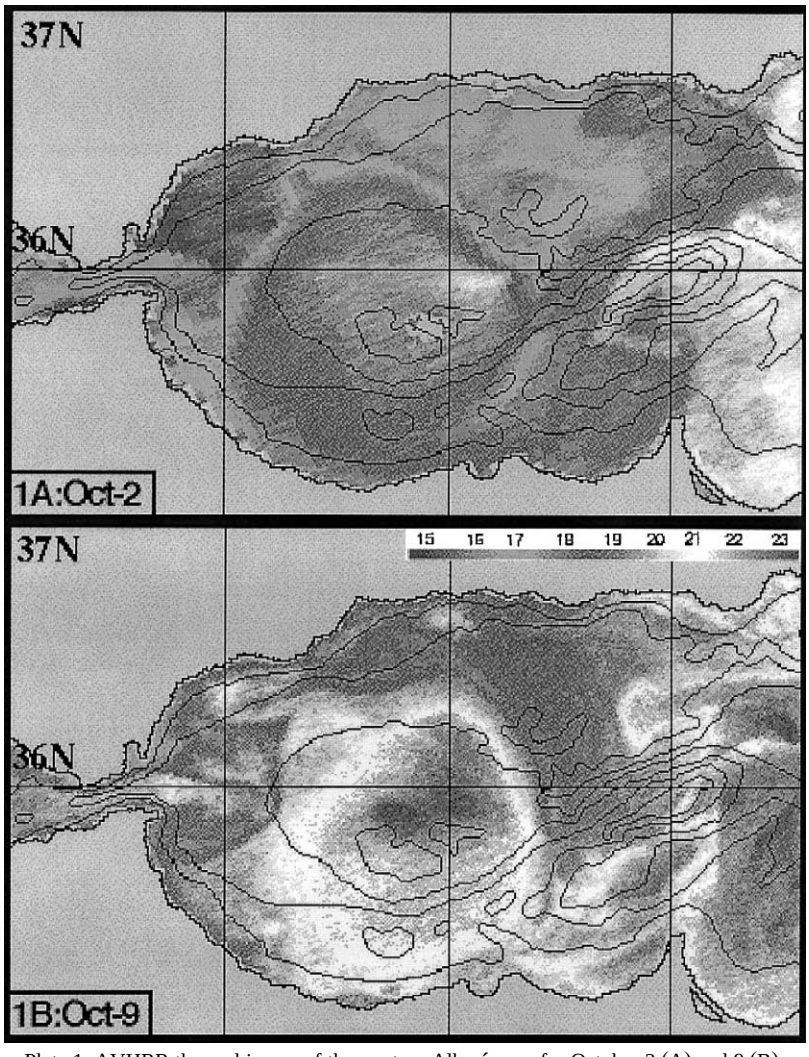

Plate 1. AVHRR thermal image of the western Alborán sea for October 2 (A) and 9 (B).

seston. The latter is related to changes in the size structure and taxonomic composition that can take place in the zone, an example which is presented in Fig. 8.

CDOM fluorescence (F_{cd}) also follows the pattern described for other variables but it has a much narrower range of variation (Fig. 9). Thus, while the lowest and highest values of c and F_{ch} differ by more than one order of magnitude, all the observed values of F_{cd} do not vary by more than a factor of two. Due to the dependence that fluorescence yield has on temperature, the observed pattern of F_{cd} could result from differences in the temperature of the water flowing through the fluorometer rather than from variations in the concentration of CDOM. There is indeed a close association between water temperature and F_{cd} during the sampling period as presented in Fig. 10. This association can result either from the response of the pelagic ecosystem to fertilization of the sea surface with deep and cold waters or from a trivial increase in quantum efficiency for fluorescence under low temperatures. The last case would invalidate our fluorometric approach to high resolution CDOM recording, and therefore

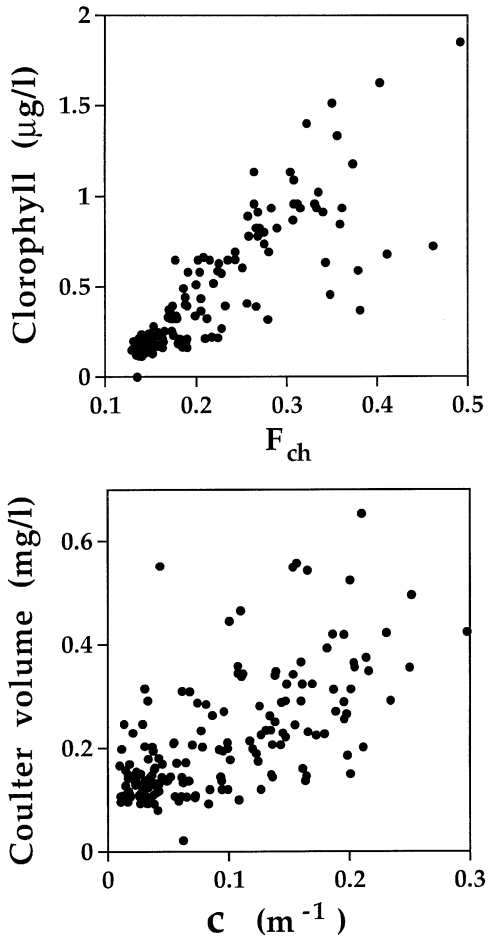

Fig. 7. Plot of chlorophyll versus F_{ch} (A) and volume of particles obtained with the Coulter Counter versus c (B).

we checked it by taking discrete samples to the laboratory, cooling them and then letting the temperature increase to room values while recording the fluorescence signal (Fig. 11). Although some decrease is observed, the variation is small when compared with that recorded during the cruise. Another possibility for our fluorometric method to produce trivial information is that F_{cd} were only the result of increasing scattering of light in the zones where particle concentration is higher. The fact that c varies by a factor of about 10 while F_{cd} factor is 2 makes clear that this is not the case. It is also evident that there is a poor correlation between both variables (Fig. 12). Moreover, CDOM absorbance in the ultraviolet is well correlated with F_{cd} (Vodacek et al., 1997). Absorbance for several filtered discrete samples was measured and a good correlation was obtained with the fluorescence signal (Fig. 13); thus, indicating the CDOM origin of F_{cd}.

4. Discussion

The existence of an anticyclonic oligotrophyc gyre and a fringe of high phytoplankton concentration at its northwestern side is a recurrent feature of the western Alborán Sea (Minas et al., 1987; Packard et al., 1988; Rubín et al., 1992; Prieto et al., 1999; Rodríguez et al., 1998; Prieto et al., in press). The persistence of this feature in the zone is consistent with statistical properties of physical variability at the whole Alborán basin. As revealed by the analysis of synoptic satellite information, almost half of the variance in the temperature and dynamic height of the surface of this basin is explained by the formation at its western side of an anticyclonic gyre associated to the entrance of the Atlantic jet (Vazquez-Cuervo et al., 1996). The jet and the gyre are quasi permanent features (Gascard and Richez, 1985; Vazquez-Cuervo et al., 1996) what makes very likely the occurrence at this zone of a situation similar to that depicted by Figs. 3–5 in which warm oligotrophic waters of the anticyclonic gyre are bordered at its north by a front of cold waters associated to the eastward jet.

The highest geostrophic Froude numbers ($Fr = N^{-2}[(\partial u/\partial z)^2 + (\partial v/\partial z)^2]$, where N is Brunt–Väisälä frequency and u and v are the zonal and meridional velocity vector components) cited for the northwestern Alborán Sea are found in a fringe that coincides with the jet at depths occupying from the surface to about 200 m (Viúdez et al., 1996). This could justify the existence of high chlorophyll fluorescence at the frontal zone by an increase in the upward flux of nutrients to the euphotic zone generated by intense vertical mixing within the jet. However, Richardson numbers ($R = 1/Fr$) in the jet, where the minima are found, are in the range of 2 to 10 (Froude numbers cited by Viúdez et al., 1996, are between 0.1 and 0.5); thus, these are higher than the value of 0.25 usually accepted for effective mixing to take place (Mann and Lazier, 1991). The high kinetic energy of the jet does not result in low

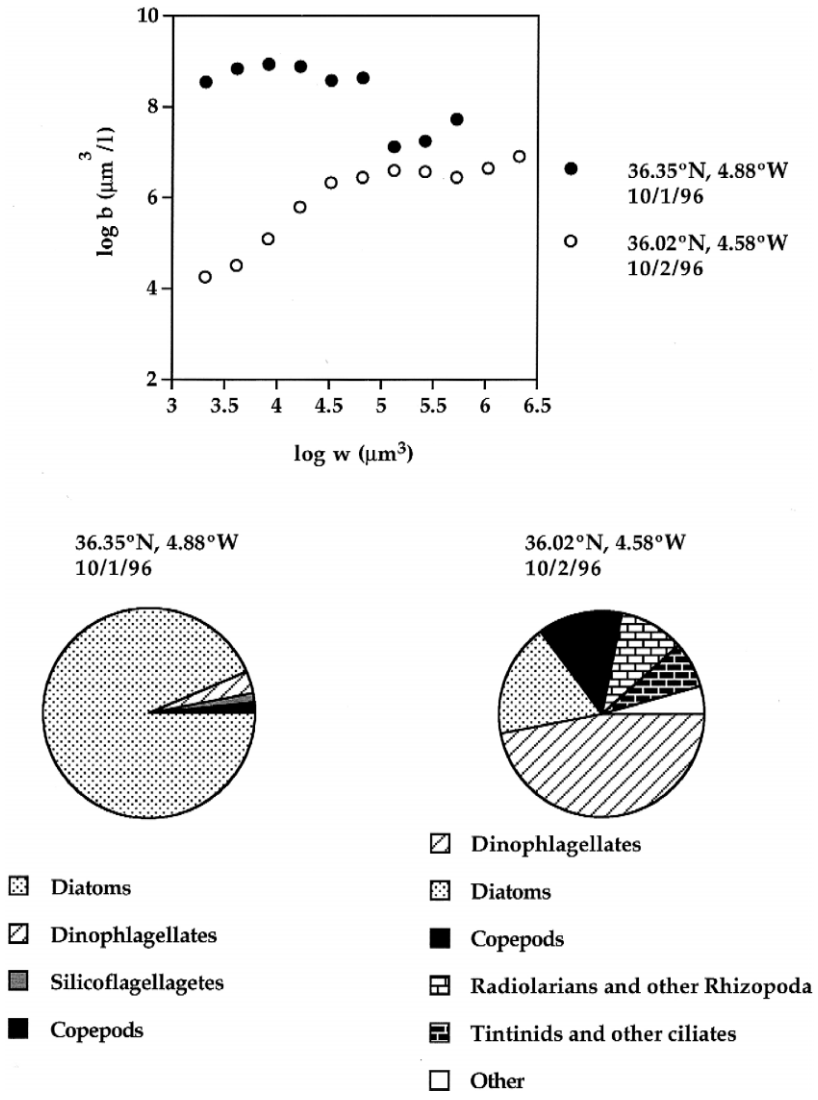

Fig. 8. Example of variations in the size spectra and taxonomic composition of plankton occupying the area. The *y*-axis is the logarithm of the total biomass of individuals contained in size classes whose upper limit is twice the size of the lower limit. Empty circles is a sample taken in day 2 of October (36.02°N; 4.58°W). Fill circles is a sample taken in day 1 of October (36.32°N; 4.88°W).

Richardson numbers because the stratification in the water column that results from both, the seasonal thermocline and the exchange of water masses in the Strait of Gibraltar, compensates for the vertical gradient of the velocity. An example of this feature is shown in Fig. 14 where water column density and velocity modulus (ADCP data) is presented for a location within the jet (36.36°N, 4.36°W) during the first survey. $R < 0.25$ do not occur despite the presence of surface velocity moduli over 1 m/s with a rapid depth decay. High R values for the jet in the Alborán Sea do note exclude the possibility of previous vertical mixing in the transit through the sills of the Strait of Gibraltar, so that surface waters in the jet could already be nutrient enriched when they enter the Alborán Sea (Gómez et al., 2000).

There also exists the possibility that high phytoplankton concentrations in the jet come from the

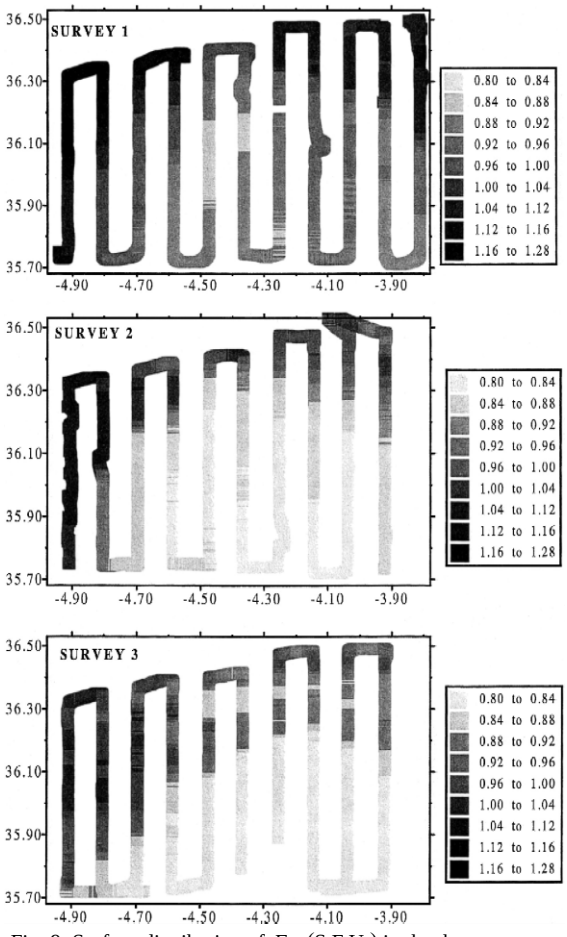

Fig. 9. Surface distribution of F_{cd} (S.F.U.) in the three surveys.

coastal upwelling at the northwestern section of our sampling area. Chlorophyll maps as shown by satellite color imagery appear to suggest this, since they depict a southward tongue of water rich in chlorophyll connected to the upwelling zone of the Spanish coast (Minas et al., 1991). La Violette (1984) observed the formation of cold submesoscale features at the northwestern part of the Alborán sea that were transported eastward with the jet. La Violette hypothesizes that chlorophyll can also be advected from this northwestern part of the Alborán sea since synoptic data from AVHRR of NOAA-7 and CZCS of Nimbus-7 images show a coincidence between low temperature and chlorophyll signal in that zone. This coastal upwelling area was scarcely sampled during the cruise, but during the first survey the

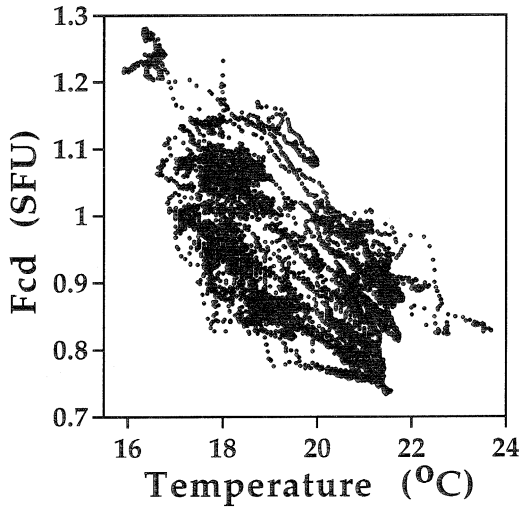

Fig. 10. Plot of F_{cd} versus temperature including all the records obtained during the three surveys.

4.92°W meridional transect depicts features similar to upwelling cores with cold and very rich in particles surface water together with the presence of very cold but biologically poor patches (Fig. 15).

Nevertheless, the analysis of water masses for this transect reveals that these patches of very cold surface water have not their origin in the upwelling area

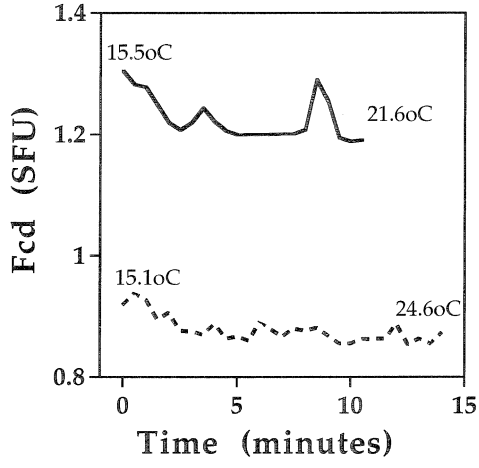

Fig. 11. Laboratory experiment to examine the effect of temperature on F_{cd}. Solid and broken lines are discrete samples from (36.23°N; 3.92°W) and (36.38°N; 4.03°W), respectively. Both samples were taken at day 11 of October. Numbers at left and right of the lines are the temperatures at the beginning and end of the time in which F_{cd} was recorded in the laboratory.

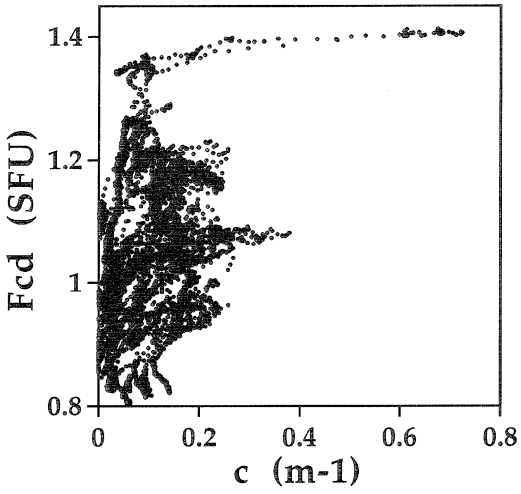

Fig. 12. Plot of F_{cd} versus c including all the records obtained during the three surveys.

but, as hypothesized by Gascard and Richez (1985), in remnants of North Atlantic Central Waters injected by the jet. Thus, Fig. 16 shows the T–S diagram of water masses above 360 m for this transect (Seasoar data). Most of the points fit to the mixture line described by Gascard and Richez (1985) for the mixing of Surface Atlantic Waters and Alborán Atlantic-Mediterranean Interface Waters, except for two sets of points termed as I and II in the figure. Both of them are surface waters but of different

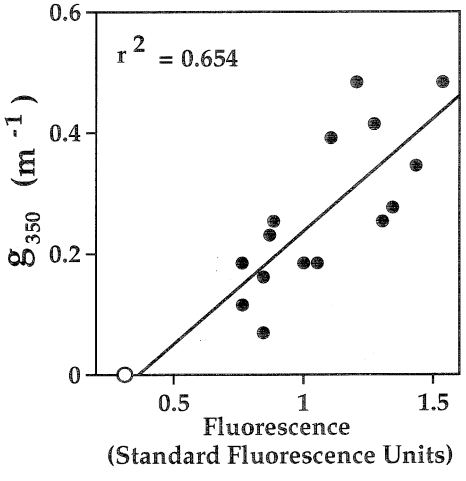

Fig. 13. Correlation between absorbance in the ultraviolet (350 nm) and F_{cd}. The empty circle is milli-Q water and is not included in the calculation of r^2.

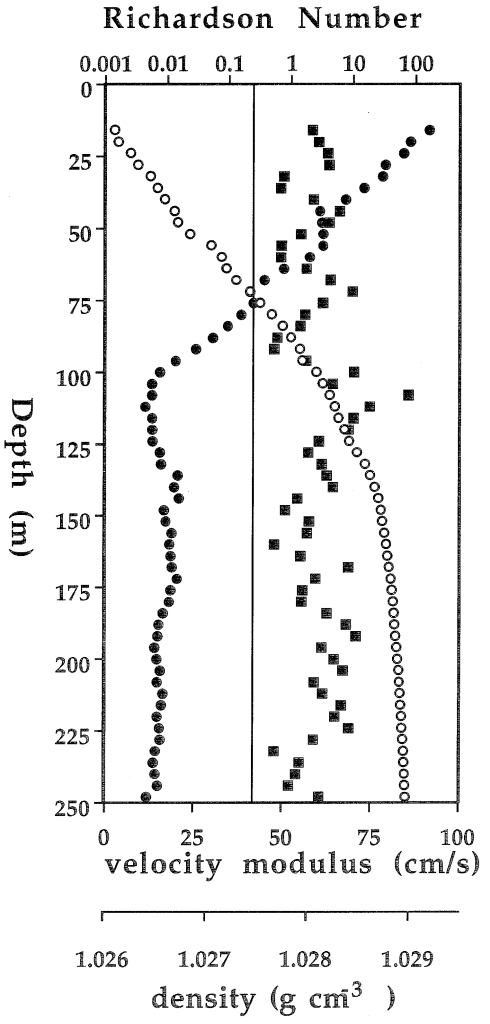

Fig. 14. Example of velocity (filled circles, ADCP data), density (empty circles, Seasoar data) and Richardson numbers (filled squares) profiles in the jet. Profile coordinates are (36.36°N, 4.36°W) and the data belong to the first survey. Vertical line shows $R = 0.25$.

origin. The first group (I) corresponds to the patches of very cold, biologically poor water apparent in Fig. 15, with T–S characteristics that denote the influence of North Atlantic Central Waters (Gascard and Richez, 1985). These have low particle concentration while in the Gulf of Cádiz because of their deep (> 100 m), below the photic zone, position in the water column. However, the incoming jet can upwell this water to the surface in the transit along the Strait of Gibraltar (Gascard and Richez, 1985). High jet

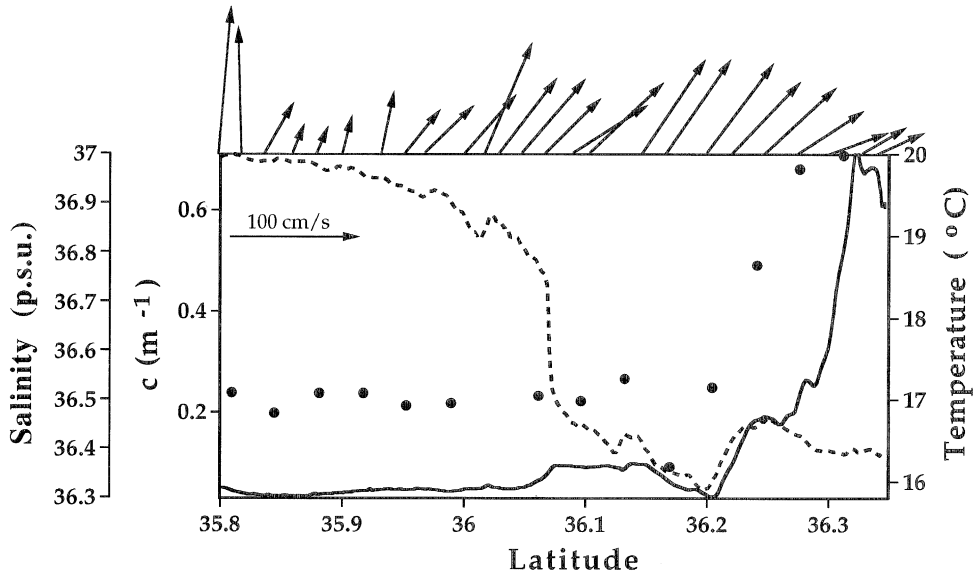

Fig. 15. Temperature (broken line) and *c* (solid line) along the south to north transect at 4.92°W during the first survey. Circles are surface salinity from Seasoar. At the top line are ADCP velocity vectors pointing upward for north and to the right for east.

velocities can transport this water to the point we detect them in the Alborán Sea before a substantial phytoplankton growth has taken place (less than 1 day). The second group (II) coincides with the very high *c* signals detected at the north end of the transect. High surface salinities denote their origin in the upwelling zone of the Spanish coast (Gascard and Richez, 1985) where lower horizontal velocities (Fig. 15) allow that high chlorophyll concentrations be found close to the place where water upwells. ADCP data does not allow to discriminate well whether or not the streamlines at this north-west (biologically rich) corner are incorporated into the jet (Fig. 17). Nevertheless, the strong spatial gradients of biological properties at this area (group I and II waters are only a few kilometers apart) reflect, to some extent, the difficulties of this counter pressure gradient transport of properties.

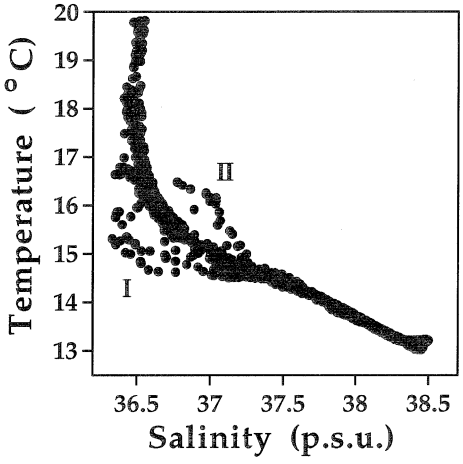

Fig. 16. *T*–*S* diagram (Seasoar data) of waters above 360 m in the 4.92°W south–north transect during the first survey.

Moreover, during the second (not shown) and third (Plate 1B) survey, AVHRR images do not depict such a clear upwelling situation for the area as in Plate 1A, but the jet is still biologically rich. This is an evidence against a possible incorporation of coastal upwelling waters as the origin of a biologically rich jet, specially during the third survey, when the jet is almost zonal (Plate 1B, Fig. 17) and the expected influence from this coastal zone is low. Finally, surface (4 to 20 m) *T*–*S* characteristics (Fig. 18, Seasoar data) of the three surveys show that most of the colder, biologically richer, waters for the sampled area do not fit to the increasing salinity with decreasing temperature pattern of the coastal upwelling (Gascard and Richez, 1985).

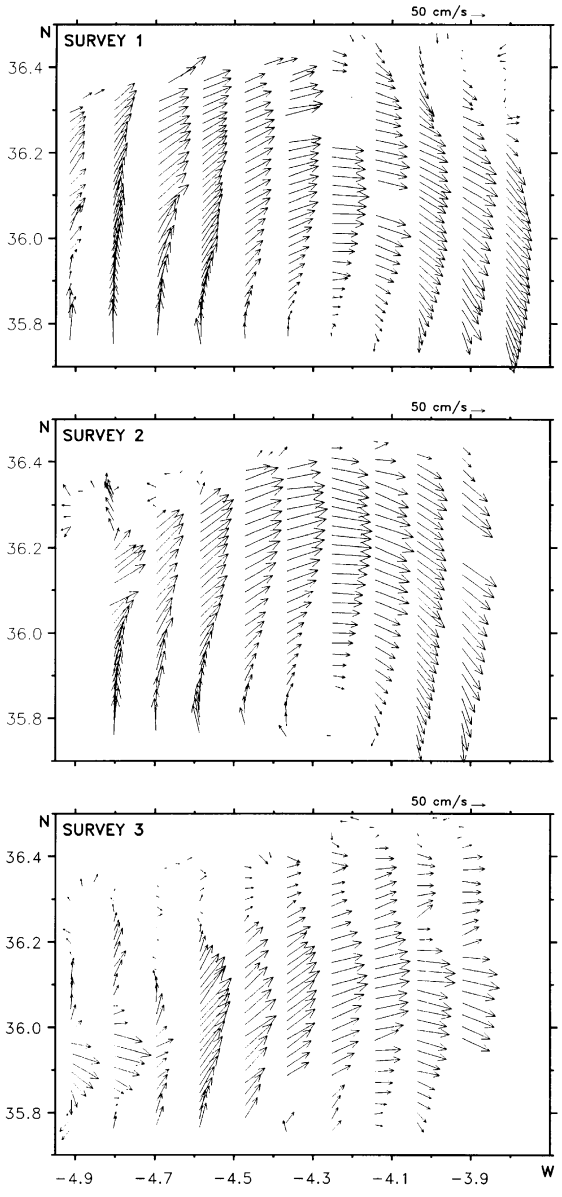

Fig. 17. ADCP surface (12 m) velocity vectors for the three surveys.

Another process that might also generate the fringe of high values of the biological signals is the ageostrophic mesoscale circulation of the area and their associated vertical velocities (Tintoré et al., 1991). Diagnosing the vertical motion through the omega equation results in intense upward velocities at the west of the survey area (Viúdez et al., 2000; Gomis et al., 2001) where an important nutrient flux to the surface can be expected. The doubling distance of phytoplankton populations in the jet is a useful calculation to analyze the origin of this biological signals in the context of the meso and macro scale circulation of the basin. This is the distance that a phytoplankton population in the jet is displaced before doubling its size. Assuming no nutrient limitation in the upwelled water, velocities between 0.4 and 1 m s^{-1} (La Violette, 1984) as well as a maximum growth rate of two doubling per day at the surface temperatures observed in the jet (Eppley, 1986) the doubling length obtained is in the range of tens to one hundred kilometers. This long length makes very improbable that upward velocities associated to ageostrophic motion (Tintoré et al., 1991) result in high local concentration of phytoplankton in the zone where the upward velocity is occurring. Moreover, if we take into account that an upwelled parcel of water is rich in nutrient but poor in cells (chlorophyll concentration in the range of 10^{-1} μg l^{-1}) the nominal distance traveled in the jet before a substantial increase in population size (chlorophyll concentration in the range of $\mu g\, l^{-1}$) has taken place is of the order of hundreds of kilometers. This spatial decoupling makes it difficult to distinguish this ageostrophic biological enrichment of the jet from

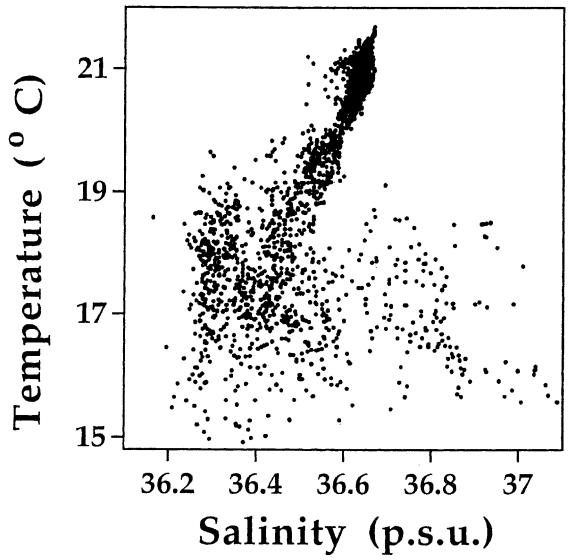

Fig. 18. $T-S$ diagram (Seasoar data) for surface (4 to 20 m) waters during the three surveys.

the abovementioned possibility of mixing at the sills of the Strait of Gibraltar. Both processes result in an input of nutrients to surface waters in the western side of the Alborán Sea but in both cases the biological response is spread within the jet along the Alborán basin.

Besides the different mechanisms considered above for the high phytoplankton concentrations in the jet, the marked differences between the surface features of surveys two and three makes clear that other processes are determining the spatial and temporal variability of phytoplankton distribution. Low frequency oscillations for the strength of the jet are known although its origin is not yet fully understood (Garret et al., 1989; Viúdez et al., 1998). Regardless of the mechanism that originates the fluctuation, this is evident in the AVHRR thermal image (Plate 1) and surface velocity field (Fig. 17) of the basin. Both reflect a situation akin to stage 2 of Viúdez et al. (1998) conceptual model for the time variability of the Atlantic jet and the Alborán gyres: the jet approaches the center of the western Alborán gyre.

Interestingly, F_{cd} follows the general pattern of temperature, chlorophyll and particles in the three surveys but with a much narrower range of variation. The close connection between F_{ch} and F_{cd} distributions suggests an autochtonous origin for the CDOM but the much narrower range of variation of the F_{cd} signal reflects a different dynamical behavior. Unfortunately, the conductivity signal of surface thermosalinograph was unstable during the cruise and prevents us to make a more precise hydrological analysis as that presented by Vodacek et al. (1997) to elucidate the CDOM origin in Middle Atlantic Bight waters. Vodacek et al. conclude that photobleaching is the main responsible for the disappearance of CDOM from surface waters, specially when, as in the Alborán Sea, these are stratified. For mid latitudes and a stratified water column Vodacek et al. calculate half lives in the range of few days for CDOM that follows the first order kinetic decay described by Miller and Zepp (1995). This can be one of the reason for a range of variation of surface CDOM which is narrower than that of particles or chlorophyll. However, the sedimentation loss of particles, and the chlorophyll associated to them, from the mixed layer also follows a first order kinetics. Moreover, the exponential coefficient for the decay of both particles and CDOM is inversely proportional to the depth of the mixed layer (H) since in the case of particles the coefficient is $-w/H$ (where w is the settling velocity) while in the case of CDOM this coefficient must depend on the light arriving at the ocean surface divided by H. The most labile dissolved organic matter in the ocean is also rapidly recycled by bacterial activity (Vodacek et al., 1997) with the generation of a refractory pool of compounds that is chemically homogeneous (Aluwihare et al., 1997). The degradation half lives for these labile high molecular weight compounds are in the range of hours–days (Amon and Benner, 1994). Therefore, the CDOM produced in the surface of the ocean is subjected to two degradation processes: photobleaching and bacterial attack. Both of them act with timescales similar or smaller to the sedimentation of particles from the mixed layer and their sum might be the origin for the narrow range of variation of F_{cd} in the Alborán Sea. In any case, it is clear that different or additional processes are controlling the distribution of CDOM when compared with particles or chlorophyll signals. This makes of the fluorometric technique developed by Hoge et al. (1993) and Vodacek et al. (1997) a valuable technique in the automatic recording of the surface waters' properties since it produces information that is not redundant with that of chlorophyll fluorescence or beam attenuation. An information that is useful in the field of remote sensing (Kirk, 1994) as well as in the studies on photosynthesis efficiency, photochemistry (Blough, 1996) and balance of heat at the surface of the ocean (Kirk, 1988).

In the case of the Alborán Sea this technique has revealed that physical processes exert a tight control on CDOM as well as on chlorophyll and particles. A control that seems to be a constant of any scale of variability analyzed: from three-dimensional macroscale spatial distribution of chlorophyll in the whole basin (Rodríguez et al., 1998) to the smaller scales associated to the Atlantic jet that we resolve in this study. This jet is the dominant physical and biological feature of the surveyed area. Although surface data are not alone enough to discriminate what physical process is forcing the biological response, ageostrophic upward velocities in the western Alborán Sea and/or mixing at the Strait of Gibraltar seem probable mechanisms for the fertiliza-

tion of a jet whose high horizontal velocities spread along the Alborán Sea the biological response to this forcing.

Acknowledgements

This work was funded by MAST project OMEGA (MAS3-CT95-0001) and by CICYT project MAR99-0643-CO3-02. The authors thank to the Omega team for their comments to the ideas included in the manuscript. We also thank the Hespérides crew and technical team for their support during the cruise. The positive criticism of anonymous reviewers on first versions of this work is acknowledged.

References

Aluwihare, L.I., Repeta, D.J., Chen, R.F., 1997. A major biopolimeric component to dissolved organic carbon in surface seawater. Nature 387, 166–169.

Amon, R.M.W., Benner, R., 1994. Rapid cycling of high-molecular-weight dissolved organic matter in the ocean. Nature 369, 549–552.

Arnone, R., Wiesenburg, D., Saunders, K., 1990. The origin and characteristics of the Algerian Current. Journal of Geophysical Research 95, 1587–1598.

Blough, N.V., 1996. Photochemistry in the sea-surface microlayer. In: Liss, P.S., Duce, R. (Eds.), The Sea Surface and Global Change. Cambridge Univ. Press, Cambridge.

Eppley, R.W. (Ed.) 1986. Plankton Dynamic of the Southern California Bight. Springer-Verlag, Berlin.

Garret, C., Akerley, J., Thompson, K., 1989. Low-frequency fluctuations in the Strait of Gibraltar from MEDALPEX sea level data. Journal of Physical Oceanography 19, 1682–1696.

Gascard, J.C., Richez, C., 1985. Water masses and circulation in the Western Alborán Sea and in the Straits of Gibraltar. Progress in Oceanography 15, 157–216.

Gómez, F., Echevarría, F., García, C.M., Prieto, L., Ruiz, L., Reul, A., Jiménez-Gómez, F., Varela, M., 2000. Microplankton distribution in the Strait of Gibraltar: coupling between organisms and hydrodynamics structures. Journal of Plankton Research 22, 603–617.

Gomis, D., Ruiz, S., Pedder, M.A., 2001. Diagnostic analysis of the 3D ageostrophic circulation from a multivariate spatial interpolation of CTD and ADCP data. Deep-Sea Research I 48, 269–295.

Hoge, F.E., Vodacek, A., Blough, N.V., 1993. Inherent optical properties of the ocean: retrival of the absorption coefficient of chromophoric dissolved organic matter from fluorescence measurements. Limnology and Oceanography 38, 1394–1402.

Kirk, J.T.O., 1988. Solar heating of water bodies as influenced by their inherent optical properties. Journal of Geophysical Research 93, 987–10908.

Kirk, J.T.O., 1994. Light and Photosynthesis in Aquatic Ecosystems. Cambridge Univ. Press, New York, 509 pp.

Lanoix, F., 1974. Etude hydrologique et dynamique de la mer d'Alboran. North Atlantic Treaty 66, 32 pp.

La Violette, P.E., 1984. The advection of submesoscale thermal features in the Alborán Sea gyre. Journal of Physical Oceanography 14, 550–565.

Mann, K.H., Lazier, J.R.N., 1991. Dynamics of Marine Ecosystems. Cambridge, 466 pp.

Miller, W.L., Zepp, R.G., 1995. Photochemical production of dissolved inorganic carbon from terrestial organic matter: significance of to the oceanic organic carbon cycle. Geophysical Research Letters 22, 417–420.

Minas, H.J., Coste, B., Minas, M., 1987. Le Detroit de Gibraltar et ses aires peripheriques: un site de forte productivite permanente. IFREMER 2e Coll. Franco-Soviétique, Yalta, 41–42.

Minas, H.J., Coste, B., Le Corre, P., Minas, M., Raimbault, P., 1991. Biological and geochemical signatures associated with the water circulation through the Strait of Gibraltar and in the western Alboran Sea. Journal of Geophysical Research 96, 8755–8771.

Packard, T.T., Minas, H.J., Coste, B., Martinez, R., Bonin, M.C., Gostan, J., Garfield, P., Christensen, J., Dortch, Q., Minas, M., Copin-Montegut, G., Copin-Montegut, C., 1988. Formation of the Alborán oxygen minimum zone. Deep-Sea Research 35, 1111–1118.

Prieto, L., García, C.M., Corzo, A., Ruiz, J., Echevarría, F., 1999. Phytoplankton, bacterioplankton and nitrate reductase activity in relation to physical structure in the northern Alborán Sea and Gulf of Cádiz. Boletin del Instituto Español de Oceanografía 15, 401–411.

Rodríguez, J., Li, W.K.W., 1994. The Size Structure and Metabolism of the Pelagic Ecosystem. Scientia Marina, Barcelona, 167 pp.

Rodríguez, J., Blanco, J.M., Jiménez-Gómez, F., Echevarría, F., Gil, J., Rodríguez, V., Ruiz, J., Bautista, B., Guerrero, F., 1998. Patterns in the size structure of phytoplankton community in the deep fluorescence maximum of the Alborán Sea (southwestern Mediterranean). Deep-Sea Research I 45, 1577–1593.

Rubín, J.P., Gil, J., Ruiz, J., Cortés, M.D., Jiménez-Gómez, F., Parada, M., Rodríguez, J., 1992. La distribución ictioplanctónica y su relación con los parámetros físicos, químicos y biológicos en el sector norte del mar de Alborán, en julio de 1991 (resultados de la campaña "Ictioalborán 0791"). Informes Técnicos del Instituto Español de Oceanografía 139.

Tintoré, J., Gomis, D., Alonso, S., Parrilla, G., 1991. Mesoscale dynamics and vertical motion in the Alborán Sea. Journal of Physical Oceanography 21, 20–823.

Vargas Yáñez, M., Sarhan Viola, T., García Lafuente, J., Cano Lucaya, N., 1999. Un modelo numérico de advección-difusión para exlicar anomalías térmicas superficiales en el cabo de Trafalgar. Boletin del Instituto Español de Oceanografía 15, 500–512.

Vazquez-Cuervo, J., Font, J., Martínez-Benjamin, J.J., 1996. Observations on the circulation in the Alborán Sea using ERS1

altimetry and sea surface temperature data. Journal of Physical Oceanography 26, 1426–1439.

Viúdez, A., Haney, R.L., Tintoré, J., 1996. Circulation in the Alborán Sea as determined by quasi-synoptic hydrographic observations: Part II. Mesoscale ageostrophic motion motion diagnosed through density dynamical assimilation. Journal of Physical Oceanography 26, 706–724.

Viúdez, A., Pinot, J.-M., Haney, R.L., 1998. On the upper layer circulation in the Alborán Sea. Journal of Geophysical Research 103, 21653–21666.

Viúdez, A., Haney, R.L., Allen, J.T., 2000. A study of the balance of horizontal momentum in a vertical shearing current. Journal of Physical Oceanography 30, 572–589.

Vodacek, A., Blough, N.V., DeGrandpre, M.D., Peltzer, E.T., Nelson, R.K., 1997. Seasonal variation of CDOM and DOC in the middle Atlantic bight: terrestial inputs and photooxidation. Limnology and Oceanography 42, 674–686.

Yentsch, C.S., Menzel, D.W., 1963. A method for the determination of phytoplankton chlorophyll and phaeophytin by fluorescence. Deep-Sea Research 10, 221–231.